The Seventh Asian-Pacific Symposium on Structural Reliability and Its Applications (APSSRA2020)
October 4–7 2020, Tokyo, Japan
T. Takada, I. Yoshida & T. Itoi (editors)

Investigation on Neural Network Model for Estimating Soil Strength by Bucket Excavation

T. Satomi[1], Y. Takahashi[2] and H. Takahashi[3]

[1]*Graduate School of Environmental Studies, Tohoku University. Email: tomoaki.satomi.c6@tohoku.ac.jp*
[2]*Graduate School of Environmental Studies, Tohoku University. Email: yusuke.takahashi.r7@dc.tohoku.ac.jp*
[3]*Graduate School of Environmental Studies, Tohoku University. Email: hiroshi.takahashi.b3@tohoku.ac.jp*

Abstract: Unmanned construction work in Japan is required because skilled people decrease and natural disasters increase in recent years. Ministry of Land, Infrastructure and Transport in Japan released "i-Construction", which is construction approach using information and communication technology (ICT) in the whole construction production processes as surveying, designing, construction and maintenance management. The current computerized construction technology uses visual information based on image of camera mounted on a vehicle body. However, the work efficiency of unmanned construction is lower than that of manned construction because visual information is not sufficient to correspond to various soil conditions. If soil strength can be estimated by using tactile information based on excavating resistive force obtained from bucket of hydraulic excavator, it can be expected that the soil strength conditions will be evaluated by in situ measurement such as computerized construction. Thus, we focus on a changing in the excavating resistive force acting on bucket influenced by the various soil types and properties. In this paper, to investigate the relationship between excavating resistive force and cone index, excavating test and portable cone penetration test were performed with various soil conditions. Then, based on the experimental data, the cone index estimation model was developed by using multilayer neural network, and the validity of the estimated results was investigated.

Keywords: ICT construction, bucket excavation, tactile information, soil strength, neural network

1. Introduction

In Japan, unmanned construction work is required because skilled people decrease and natural disasters increase. Ministry of Land, Infrastructure and Transport in Japan (2015) released "i-Construction", which is construction approach using information and communication technology (ICT) in the whole construction production processes as surveying, designing, construction and maintenance management. The current computerized construction technology uses visual information based on image of camera mounted on a vehicle body. However, the work efficiency of unmanned construction is lower than that of manned construction because visual information is not sufficient to correspond to various soil conditions: types, densities and water contents, and so on. If soil strength parameters such as cone index, cohesion, and internal friction angle can be estimated using tactile information such as excavating resistive force acting on blade of bulldozer or bucket of hydraulic excavator, it becomes possible that the soil strength is evaluated at a construction site.

Previous studies on estimation of cohesion and internal friction angle of soil using a model for predicting excavating resistive force acting on bucket or blade have been reported (Tan et al. 2005a, 2005b, Moghaddam et al. 2012). The two main features of these developed techniques are that (1) limit equilibrium methods such as Mohr-Coulomb model are adopted to predict the failure force and (2) the unknown soil parameters are estimated as to minimize the error between the measured failure force and the modeled one. Moreover, to estimate the unknown soil parameters, the number of the measured force with different angles of excavator tool needs to be the same as the number of the unknown soil parameters. Thus, the estimating accuracy of the soil parameters by the above developed method depends on the soil excavation model. However, since the soil cutting patterns differ according to the kinds of soil and the failure conditions of soil (Hatamura and Chijiiwa 1975), the soil excavation model needs to correspond to various soil types and properties.

Based on the above backgrounds, we focus on a changing in excavating resistive force acting on bucket influenced by the various soil types and properties. Fig. 1 shows outline of proposed method for estimating soil strength parameters by excavator bucket. The proposed method is based on a machine learning utilizing experimental data and numerical simulation data. The final goal of this study is to establish estimation method of soil strength parameters using excavator bucket. In this paper, a cone index estimation model for evaluating soil strength and terrain trafficability is developed using all laboratory experimental data. Specifically, laboratory

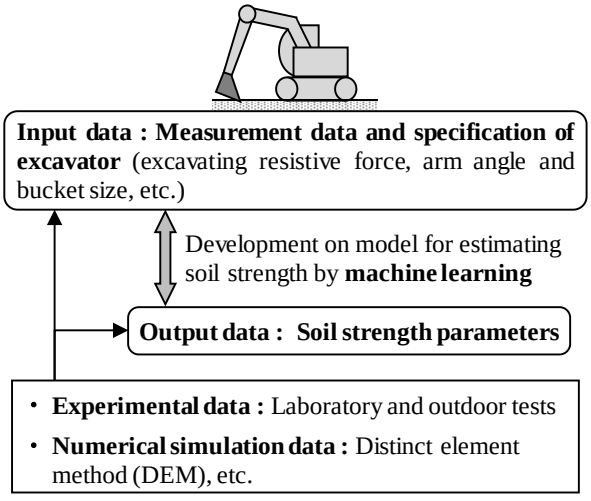

Figure 1. Outline of proposed method for estimating soil strength by excavator bucket.

excavation test and portable cone penetration test are performed with various soil conditions. Moreover, based on the obtained experimental data, the cone index estimation model is developed using multilayer neural network that is one of machine learning techniques because the multilayer neural network is effective for developing the non-linear relationship, and the validity of the estimated values is investigated.

2. Laboratory Tests

2.1 Outline of laboratory tests

The excavating test to measure the excavating resistive force acting on bucket and portable cone penetration test to measure cone index were performed with various soil conditions, i.e., soil type, water content and density. Table 1 shows the laboratory test conditions and the laboratory tests were carried out by combining the conditions shown in Table 1. Fig. 2 shows the grain size distribution curve of each soil. In a series of tests, soil sample was silica sand (soil particle density ρ_s = 2.65 Mg/m^3) mixed with Kasaoka clay (typical kaolin clay, ρ_s = 2.74 Mg/m^3). As shown in Table 1, the soil type was from sandy soil to clayey soil, the soil water content state was from relatively dry to wet conditions, and the dry density was set to within the range that specimen can be created. The oven-dried soil was mixed with water that is adjusted to be a given water content. After that, the soil samples were compacted to be a given dry density.

Fig. 3 shows soil excavation test apparatus. The test apparatus consists of a DC motor, a force sensor, a triangular prism-shaped bucket of (length: 54 mm, width: 58 mm, height: 54 mm) and a soil box (length: 346mm, width: 126mm, height: 48mm). The bucket moves along the circular track, as shown in Fig. 4. The maximum excavating depth D was set to 15 mm. The radius R was 206 mm which is distance between the base of the arm and the blade tip of the bucket. The arm angle θ was calculated based on the motor rotating angular speed. The excavating speed was set to 5.3 deg/s. The data sampling frequency was set to 10 Hz.

The portable cone penetration test was conducted based on Japanese Geotechnical Society Standards (JGS1431) using a vinyl chloride resin cylindrical container (Diameter: 108 mm, Height: 180 mm). The penetration resistance under the depth of 100 mm was measured, and cone index was determined dividing the penetration resistance by the cone base area.

The excavating tests and the cone penetration tests were conducted three or four times on each test condition. The average values were used for learning by multilayer neural network.

2.2 Experimental results and discussions

Fig. 5 shows examples of measurement result of soil excavation test. As shown in Fig. 5, since it seems that the peaks "+" correspond to the soil failure by bucket, this study focused on five index parameters; (1) excavating resistive force of first soil failure F_{f1}, (2) arm angle θ_{f1} corresponding to F_{f1}, (3) excavating work to reach first soil failure W_{f1}, (4) maximum excavating resistive force F_{max} and (5) total excavating work W. F_{f1} is determined

Table 1. Laboratory test conditions.

Parameter	Condition
Mixing ratio of sand to clay s/c	1/0, 3/1, 1/1, 1/3, 0/1
Water content w [%]	5, 10, 15, 20, 25, 30
Dry density ρ_d [Mg/m^3]	1.0, 1.1, 1.2, 1.3

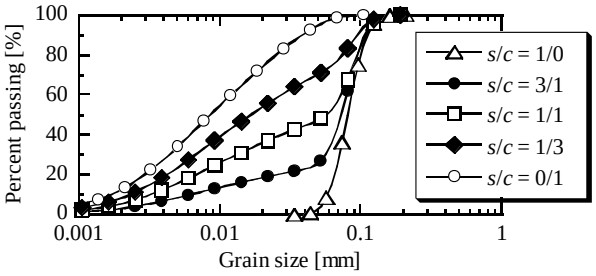

Figure 2. Grain size distribution curve of each soil.

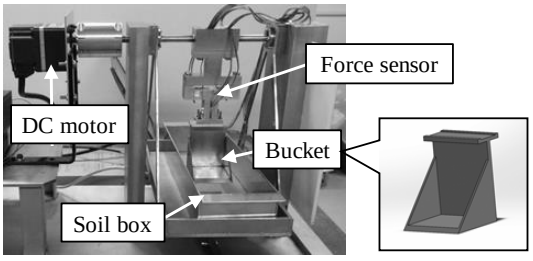

Figure 3. Soil excavation test apparatus.

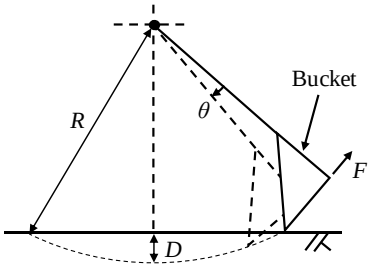

Figure 4. Track of excavator bucket.

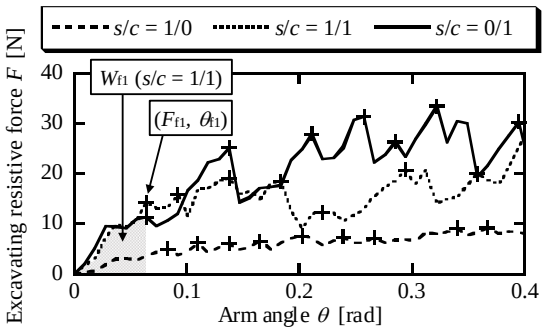

Figure 5. Examples of measurement results of soil excavation tests (w = 15% and ρ_d = 1.2 Mg/m^3).

when $[F(\theta_{t-2}) < F(\theta_t) \cap F(\theta_{t-1}) < F(\theta_t) \cap F(\theta_t) > F(\theta_{t+1})]$ or $[F(\theta_{t-N}) < F(\theta_t) \cap F(\theta_t) > F(\theta_{t+N})$ $(N = 1, 2)]$ is satisfied, where $F(\theta_t)$ is the excavating resistive force at the t-th arm angle θ. The excavating work W_{f1} corresponds to workload from the start of excavation to the first soil failure, and the grey area in Fig. 5 indicates

the excavating work W_{f1}. The maximum excavating resistive force F_{max} is the maximum force during excavation. The total excavating work W corresponds to workload from the start to the end of excavation.

Fig. 6 shows relationship between excavating index parameters (i.e., F_{f1}, W_{f1} and F_{max}) and cone index. As shown in Fig. 6, the cone index decreased with increasing F_{f1}, W_{f1} and F_{max}, although there were variations in the results. Moreover, for example, the symbol "○" in Fig. 6 shows the results obtained under the constant values of soil type and dry density and different water contents. The results indicated that cone index, F_{f1}, W_{f1} and F_{max} increased with increasing dry density. On the other hand, the symbol "■" in Fig. 6 shows the results obtained under the constant values of soil type and dry density and different water contents. The results indicated that cone index decreased and F_{f1}, W_{f1} and F_{max} increased with increasing water content. Thus, it was observed that cone index was affected by soil properties. From the above results, it was found that the excavating resistive force and cone index are the integrated index values of soil mechanics changed by soil properties. Moreover, the relationship between cone index and excavating index parameter was nonlinear and was not clearly a one-to-one relationship. Therefore, it seems possible to estimate cone index from soil excavation work using multilayer neural network.

3. Learning by Multilayer Neural Network

3.1 Outline of multilayer neural network

Fig. 7 shows basic structure and learning process of the multilayer neural network using back propagation algorithm (Rumelhart et al. 1986a, 1986b). The back propagation is a supervised learning algorithm which takes input values and target values in advance and generally consists of input layer, hidden layer and output layer, as shown in Fig. 7. The input-output relationships of hidden layer and output layer are expressed as Eq. 1.

$$y_j = f\left(\sum_{i=1}^{L} x_i w_{ij} + b_j\right), \quad z_k = f\left(\sum_{j=1}^{M} y_j v_{jk} + b_k\right) \qquad (1)$$

where x_i is input value of neuron i, y_j is output value of neuron j, z_k is output value of neuron k, b_j is threshold of neuron j, b_k is threshold of neuron k, w_{ij} is weight between neuron i and neuron j, v_{ij} is weight between neuron j and neuron k and $f(\cdot)$ is activation function of neuron.

The activation functions of hidden layer are sigmoid function and Rectified linear unit (ReLU) function (Nair and Hinton 2010, Glorot et al. 2011), and so on. On the other hand, the activation function of output layer is identity function, and the number of output layer k is one because the case of this study is a regression problem for estimating cone index.

The weights $\mathbf{w}$ (i.e., w_{ij}, v_{ij}) in Fig. 7 are renewed to find the minimum of error E between output value calculated from the network and target value by using optimization algorithm of weights such as gradient descent method with momentum (Rumelhart et al. 1986a) and Adam (Kingma and Ba 2014).

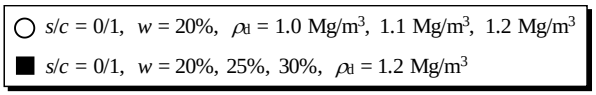

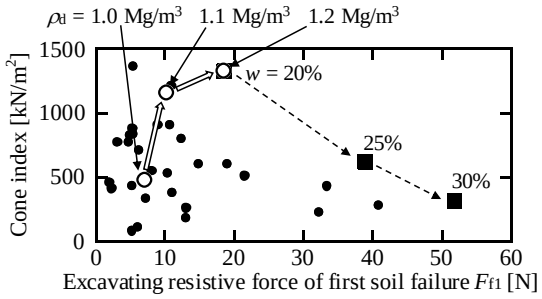

(a) Excavating resistive force F_{f1} ~ cone index

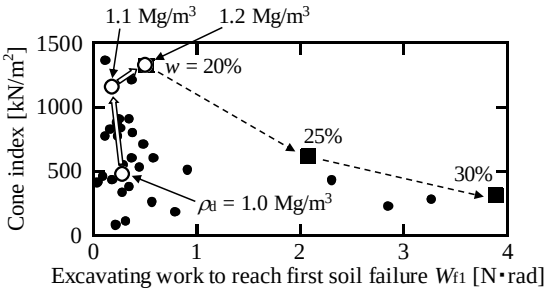

(b) Excavating work W_{f1} ~ cone index

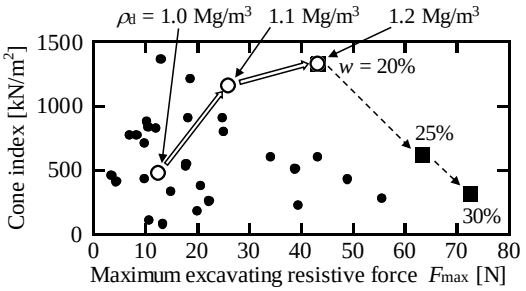

(c) Maximum excavating resistive force F_{max} ~ cone index

Figure 6. Examples of relationship between excavating index parameter between cone index.

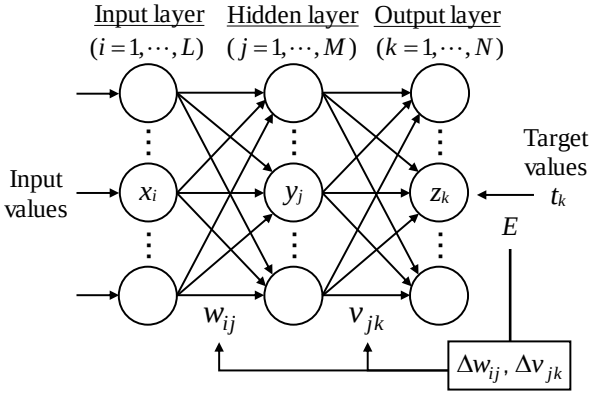

Figure 7. Basic structure and learning process of multilayer neural network using back propagation algorithm.

3.2 Learning conditions

To develop the neural network model for estimating cone index from soil excavation by bucket, it is necessary to set and input various parameters, i.e., 1) input and output variables, 2) the number of neurons for the hidden layer, 3) activation function for hidden layer, 4) optimization of weights, 5) initial values of weights and 6) learning steps. The learning conditions in this paper are described below, and Table 2 summarizes the learning conditions.

The learning was conducted with different the number of input variables in order to compare the learning performance of multilayer neural network. Before the learning, the log-transformation of input values was conducted, and the input values were standardized to have a mean of zero and a standard deviation of one. On the other hand, the log-transformation and standardization of output values were not conducted.

When the number of neurons for hidden layer M increases, a generalization capability of non-learning data decreases. Therefore, the maximum M was set to the number that is three times the number of neurons for input layer according to Hush (1989), and the learning was conducted with different the number of neurons.

To compare the learning performance of multilayer neural network, sigmoid function conventionally used in multilayer neural network (see Eq. 2) and Rectified linear unit (ReLU) function (see Eq. 3, Nair and Hinton 2010, Glorot et al. 2011) used in the current neural network were used as the activation function $f(x)$.

$$f(x) = \frac{1}{1+e^{-x}} \tag{2}$$

$$f(x) = \begin{cases} 0 & (x \le 0) \\ x & (x > 0) \end{cases} \tag{3}$$

where x is weighted sum of hidden layer, and is corresponding to the value in the parenthesis of Eq. 1.

The two learning optimization algorithms of weights for finding minimum of the error were used in order to compare the learning performances of neural network. Specifically, the gradient descent method with momentum (see Eq. 4, Rumelhart et al. 1986a, and hereinafter referred to as Momentum) used in the current neural network and the Adam (see Eq. 5, Kingma and Ba 2014) used in the current neural network were selected.

$$\mathbf{w}(t+1) = \mathbf{w}(t) - \eta \nabla E(\mathbf{w}(t)) + \alpha \Delta \mathbf{w}(t-1) \tag{4}$$

where t is learning step, η is learning rate and α is momentum decay factor ($0 < \alpha < 1$). η and α are set to 0.1 and 0.9, respectively, according to Rumelhart et al (1986a).

$$\begin{aligned} \mathbf{m}(t+1) &= \beta_1 \cdot \mathbf{m}(t) + (1-\beta_1) \cdot \nabla E(\mathbf{w}(t)) \\ \mathbf{v}(t+1) &= \beta_2 \cdot \mathbf{v}(t) + (1-\beta_2) \cdot \nabla E(\mathbf{w}(t))^2 \\ \mathbf{w}(t+1) &= \mathbf{w}(t) - \eta \cdot \frac{\mathbf{m}(t+1)}{1-\beta_1^t} \cdot \frac{1}{\sqrt{\frac{\mathbf{v}(t+1)}{1-\beta_2^t}} + \varepsilon} \end{aligned} \tag{5}$$

Table 2. Learning conditions.

Parameter	Condition
Input variables	Case1: F_{f1}, θ_{f1}, W_{f1}, F_{max}, W
	Case2: F_{f1}, θ_{f1}, W_{f1}, F_{max}
	Case3: F_{f1}, θ_{f1}, W_{f1}, W
Target variable	Cone index
Number of neurons for hidden layer	Case1: 5 ~ 15
	Case2: 4 ~ 12
	Case3: 4 ~ 12
Activation function for hidden layer and optimization	Case1: Sigmoid–Momentum
	Case2: ReLU–Adam
Initial values of weights	Sigmoid: $-\sqrt{\frac{1}{n}} < \mathbf{w} < \sqrt{\frac{1}{n}}$
	ReLU: $-\sqrt{\frac{2}{n}} < \mathbf{w} < \sqrt{\frac{2}{n}}$
	where n is the number of the preceding layer.
	$\mathbf{w} = 0$ (threshold)
Learning steps	Learning steps when MSE of non-learning data is minimized

where t is learning step, η is learning rate, β_1 and β_2 are momentum decay rates and ε is smoothing term. β_1, β_2 and ε were set to 0.9, 0.999 and 10^{-8}, respectively, according to Kingma and Ba (2014).

The initial values of weights were set to random number according to activation function for hidden layer based on Glorot and Bengio 2010 and He et al. 2015. The initial value of threshold was set to zero. In general, since the learning result is affected by the initial values of weights, the learning with changing the initial values of weights was conducted, and the average of learning result was calculated.

When the learning steps increase, the error becomes small. However, since the learning becomes over fitting, the generalization capability of neural network model for non-learning data decreases. Thus, the all experimental data were randomly separated into learning data (80% of all data) and non-learning data (20%), and the learning was stopped when the error of non-learning data was minimized. Mean squared error (MSE, see Eq. 6) was used as the error function E.

$$MSE = \frac{1}{N}\sum_{p=1}^{N}\left(z_p - t_p\right)^2 \tag{6}$$

where z_p is output value of the p-th training data and t_p is the p-th target value and N is the size of data.

3.3 Learning results and discussions

Fig. 8 shows the learning results accumulated MSEs of learning data and non-learning data with various learning conditions. Specifically, Fig.8 (a1, a2, a3) indicate the learning results in case of with different input variables and using sigmoid activation function and Momentum as learning optimization. Fig.8 (b1, b2, b3) indicate the learning results in case of with different input

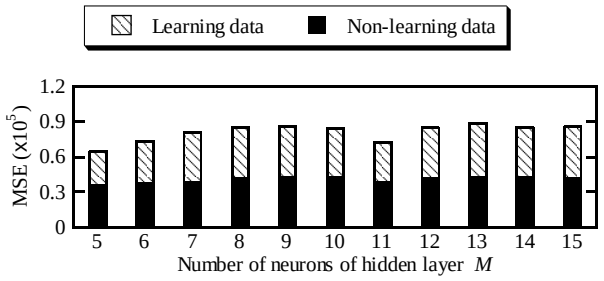

(a1) Five variables (F_{f1}, θ_{f1}, W_{f1}, F_{max}, W), Sigmoid-Momentum

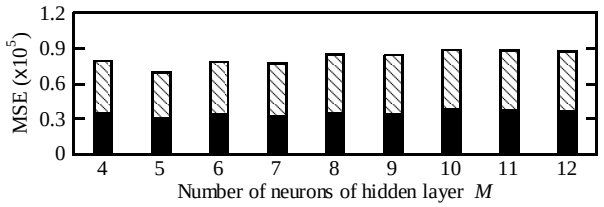

(a2) Four variables (F_{f1}, θ_{f1}, W_{f1}, F_{max}), Sigmoid-Momentum

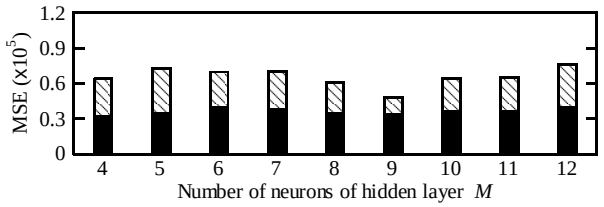

(a3) Four variables (F_{f1}, θ_{f1}, W_{f1}, W), Sigmoid–Momentum

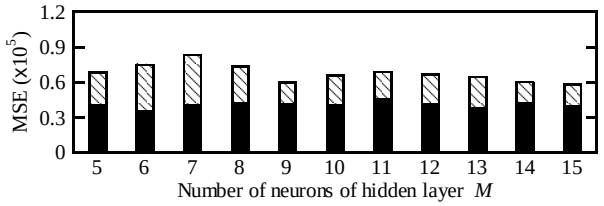

(b1) Five variables (F_{f1}, θ_{f1}, W_{f1}, F_{max}, W), ReLU-Adam

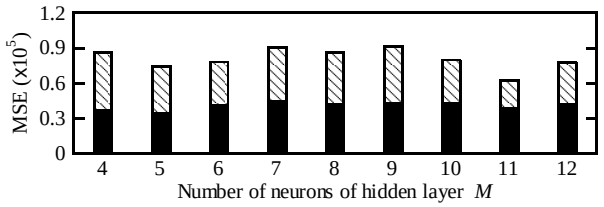

(b2) Four variables (F_{f1}, θ_{f1}, W_{f1}, F_{max}), ReLU-Adam

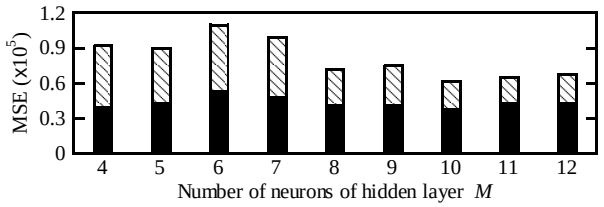

(b3) Four variables (F_{f1}, θ_{f1}, W_{f1}, W), ReLU-Adam

Figure 8. Relationship between the number of neurons of hidden layer and MSE with various learning conditions.

variables and using ReLU activation function and Adam as learning optimization.

As shown in Fig. 8, the accumulated MSE changed with increasing the number of neurons of hidden layer, and the number of neurons of hidden layer with the smallest accumulated MSE existed. Moreover, in the case of "Sigmoid-Momentum", the MSE of the four input variables with total excavating work W, as shown in Fig. 8 (a3), was smaller than the MSEs of the other input variables. On the other hand, in the case of "ReLU-Adam", the MSE of the five input variables, as shown in Fig. 8 (b1), was smaller than the MSEs of the other input variables. From the results, it can be seen that there are an appropriate activation function and optimization depending on the input variables, i.e., a neural network model. Thus, in the condition ranges of this study, the most commonly used neural networks with ReLU as the activation function and Adam as the optimization, are not necessarily the most suitable, and the MSE is not necessarily smaller with increasing number of input variables.

Focusing on the smallest accumulated MSE in all cases, the neural network learning conditions with four input variables (i.e., F_{f1}, θ_{f1}, W_{f1} and W), nine neurons of hidden layer, the sigmoid as activation function, and Momentum as optimization, were the most suitable for estimating cone index from soil excavation work, and Table 3 summarizes the optimum learning conditions.

Fig. 9 shows the comparison between the measured cone index and the estimated cone index. The estimated cone index was obtained from the neural network learning conditions shown in Table 3. As shown in Fig. 9, cone index was estimated with accuracy of the measured value ± 300 kN/m^2 at maximum. Thus, by using the multilayer neural network, the cone index was able to be

Table 3. Optimum learning conditions

Parameter	Condition
Input variables	F_{f1}, θ_{f1}, W_{f1}, W
Number of neurons for hidden layer	9
Activation function for hidden layer	Sigmoid
Optimization	Momentum

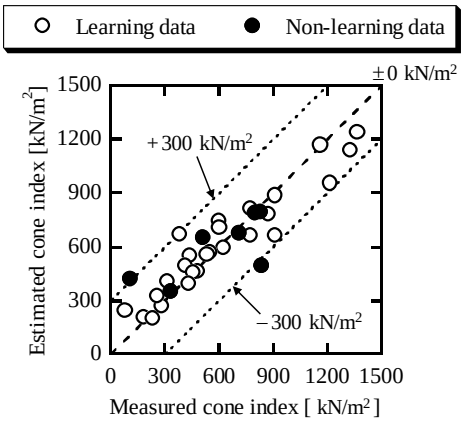

Figure 9. Comparison between estimated cone index and measured cone index.

estimated through soil excavation by bucket.

4. Conclusions

In this paper, firstly, excavation tests and portable cone penetration tests were performed with various soil conditions, and excavating resistive force and cone index were measured, respectively. After that, by utilizing the experimental data obtained, the cone index estimation model with multilayer neural network was developed. The following results were obtained.

The excavating resistive force and cone index were the integrated index values of soil mechanics changed by soil properties such as density and water content. Moreover, the relationship between cone index and excavating resistive force by bucket was nonlinear and was not clearly a one-to-one relationship.

The developed multilayer neural network had an appropriate activation function and optimization depending on the input variables, i.e., the neural network model in the condition ranges of this study. Focusing on the smallest accumulated MSE, the neural network learning conditions with four input variables (i.e., F_{f1}, θ_{f1}, W_{f1} and W), nine neurons of hidden layer, the sigmoid as activation function and Momentum as optimization, were the most suitable for estimating cone index from soil excavation work. By using the developed neural network model, the cone index was estimated with accuracy of the measured value ± 300 kN/m^2 at maximum.

Future works for experiment are carried out with different sizes of excavator bucket and the ununiformed soil containing gravel in order to storage and update data and to further investigate estimation model for cone index through soil excavation. Since the structure of neural network used in this paper was the simplest, it is necessary to further investigate the structure of neural network such as adding the number of hidden layers. Moreover, investigation using other machine learning techniques is also required.

Acknowledgment

This work was supported by JSPS KAKENHI Grant Number JP19K04592.

References

Glorot, X. and Bengio, Y., 2010. Understanding the difficulty of training deep feedforward neural networks, *Proceedings of the Thirteenth International Conference on Artificial Intelligence and Statistics*, 249–256.

Glorot, X., Bordes, A., and Bengio, Y., 2011. Deep sparse rectifier neural networks. AISTATS'11, *Proceedings of the 14th International Conference on Artificial Intelligence and Statistics*, 15: 315–323.

Hatamura, Y. and Chijiiwa, K., 1975. Analysis of the mechanism of soil: 1st Report. Cutting patterns of soils, *Bulletin of JSME*, 18(120): 619–626.

He, K., Zhang, X., Ren, S. and Sun, J., 2015. Delving Deep into Rectifiers: Surpassing Human-Level Performance on ImageNet Classification, *Proc. of the IEEE International Conference on Computer Vision (ICCV)*, 1026–1034.

Hush, D.R., 1989. Classification with neural networks: a performance analysis, *Proc. of the IEEE International Conference on Systems Engineering*, 277–280.

Ministry of Land, Infrastructure and Transport in Japan, http://www.mlit.go.jp/tec/i-construction/index.html (in Japanese) (accessed 2020-5-11).

Moghaddam, R.Y., Kotchon, A. and Lipset, M.G., 2012. Method and apparatus for on-line estimation of soil parameters during excavation, *J. Terramechanics*, 49(3,4): 173–181.

Nair, V. and Hinton, G.E., 2010. Rectified Linear Units Improve Restricted Boltzmann Machines. *Proc. of the 27th International Conference on Machine Learning*, (3): 807–814.

Rumelhart, D.E., Hinton, G.E. and Williams, R.J., 1986a. Learning representations by back-propagating errors, *Nature*, 323(99), 533–536.

Rumelhart, D.E. and McClelland, J.L., the PDP Research Group, 1986b. Parallel Distributed Processing, MIT Press.

Tan, C., Zweiri, Y.H., Althoefer, K. and Seneviratne, L.D., 2005a. On-line soil parameter estimation scheme based on newton raphson method for autonomous excavation, *IEEE/ASME Transactions on Mechatronics*, 10(2): 221–229.

Tan, C., Zweiri, Y.H., Althoefer, K. and Seneviratne, L.D., 2005b. Online soil-bucket interaction identification for autonomous excavation, *Proc. 2005 IEEE International Conference on Robotics and Automation*, 3576–3581.